Published in final edited form as:
Am J Transplant. 2010 February ; 10(2): 231–241. doi:10.1111/j.1600-6143.2009.02930.x.

RGS4 Controls Renal Blood Flow and Inhibits Cyclosporine-Mediated Nephrotoxicity

Andrew Siedlecki[1,2], **Jeff R. Anderson**[3], **Xiaohua Jin**[1], **Joel R. Garbow**[4], **Traian S. Lupu**[1], and **Anthony J. Muslin**[1,2,5]

[1]Center for Cardiovascular Research, John Milliken Department of Internal Medicine, Washington University School of Medicine, St Louis, MO 63110.

[2]Nephrology Division, John Milliken Department of Internal Medicine, Washington University School of Medicine, St Louis, MO 63110.

[3]Department of Chemistry, Washington University School of Medicine, St Louis, MO 63110.

[4]Biomedical Magnetic Resonance Laboratory, Mallinckrodt Institute of Radiology, Washington University School of Medicine, St Louis, MO 63110.

[5]Department of Cell Biology and Physiology; Washington University School of Medicine, St Louis, MO 63110.

Abstract

Calcineurin inhibitors (CNI) are powerful immunomodulatory agents that produce marked renal dysfunction due in part to endothelin-1-mediated reductions in renal blood flow. Ligand-stimulated Gq protein signaling promotes the contraction of smooth muscle cells via phospholipase Cβ-mediated stimulation of cytosolic calcium release. RGS4 is a GTPase activating protein that promotes the deactivation of Gq and Gi family members. To investigate the role of G protein-mediated signaling in the pathogenesis of CNI-mediated renal injury, we used mice deficient for RGS4 (*rgs4*$^{-/-}$). Compared to congenic wild type control animals, *rgs4*$^{-/-}$ mice were intolerant of the CNI, cyclosporine (CyA), rapidly developing fatal renal failure. *Rgs4*$^{-/-}$ mice exhibited markedly reduced renal blood flow after CyA treatment when compared to congenic wild type control mice as measured by magnetic resonance imaging (MRI). Hypoperfusion was reversed by coadministration of CyA with the endothelin antagonist, bosentan. The MAPK/ERK pathway was activated by cyclosporine administration and was inhibited by cotreatment with bosentan. These results show that endothelin-1-mediated Gq protein signaling plays a key role in the pathogenesis of vasoconstrictive renal injury and that RGS4 antagonizes the deleterious effects of excess endothelin receptor activation in the kidney.

Introduction

Vascular smooth muscle cells regulate renal blood flow depending on their contractile state[1]. Extracellular ligands, such as endothelin-1 and angiotensin II, regulate vascular tone by binding to transmembrane receptors on smooth muscle cells[2, 3]. Calcineurin inhibitors were first demonstrated to induce renal vasoconstriction through the endothelin receptor by Lanese and colleagues [4]. Several ligands thought to play a critical role in the regulation of vascular tone bind to seven transmembrane receptors (STRs), also called G protein coupled receptors (GPCRs)[5]. When endothelin-1 binds to the endothelin type A

Correspondence to: Dr. Anthony J. Muslin, 660 South Euclid Avenue, Campus Box 8086, St. Louis, MO 63110 USA; amuslin@dom.wustl.edu; Phone : 314-747-3525 ; Fax: 314-747-3545.

(ET-A) GPCR, activated Gαq, finally stimulates cytosolic calcium levels to increase promoting contraction of smooth muscle cells[6, 7]. The Gq-coupled adrenergic receptor is also capable of phosporylating ERK1/2 in vascular smooth muscle cells[8–11]. This signaling pathway promotes the metabolic adaptation to increased mechanical load [8, 12]

Regulator of G protein signaling (RGS) proteins are a family of GTPase activating proteins for heterotrimeric G proteins[13, 14]. They are differentially expressed in the renal cortex and medulla and include RGS1, RGS2, RGS4, and RGS13 [15]. RGS4 is a small RGS protein that consists of an amino-terminal polybasic region and a single RGS core domain. It has GAP activity towards both Gi and Gq proteins when tested in vitro and in vivo[13, 14]. Its amino terminal sequence contains an N-degron degradation signal which targets the protein for proteasomal degradation [16]. RGS4 mRNA expression is present in both the cortex and the medulla, however the inner and outer medulla of the human kidney have relatively increased levels of expression [21].

Calcineurin inhibitors (CNI) are powerful immunomodulatory agents that are used by 98% of renal transplant recipients [17] to prevent transplant rejection, but often cause marked renal dysfunction[18]. Several hypotheses seek to explain the mechanism of acute cyclosporine toxicity [19], including oxidant stress [20, 21], the renin-angiotensin-aldosterone system [22], nitric oxide inhibition [23], and enhancement of endogenous ligands to GPCRs [24].

A longstanding explanation of acute cyclosporine renal toxicity is that cyclosporine-triggered endothelin-1 release by vascular endothelial cells promotes renal vasoconstriction and reduced renal blood flow [4, 25, 26]. Albig and Schiemann showed that RGS4 overexpression in endothelial cells prevented endothelin from activating extracellular signal-regulated kinase (ERK1/2)[27]. Therefore, we proposed that RGS4 might play a critical role in limiting acute renovascular smooth muscle cell Gq activation after endothelin-1 release by endothelial cells. To test this model, mice deficient for RGS4 were generated and treated with cyclosporine. RGS4-deficient mice were highly sensitized to cyclosporine-induced renal failure and reduced renal blood flow.

Materials and Methods

Targeted disruption of the rgs4 gene

Murine 129/SvJ embryonic stem cells with targeted disruption of one allele of the *rgs4* gene were generated. The details of this procedure are found in the online supplemental data.

Cell culture

Kidneys from *rgs4*$^{-/-}$ and congenic wild type control mice were procured after injecting mice with pentobarbital (0.05 mg/g). Tissue was washed in 10 mM PBS, cut in 2 mm sections, and plated in endothelial cell media (Cell Applications, Inc., San Diego, CA) pretreated with endothelin (0.25 μM) (Sigma Aldrich; St. Louis, MO) or cyclosporine (20 μg/mL) (Sigma Aldrich; St. Louis, MO). Tissue was then processed after a 10 minute incubation time.

Nephrectomy followed by Cyclosporine A and/or Bosentan Treatment in Mice

All research involving the use of mice was performed in strict accordance with protocols approved by the Animal Studies Committee of Washington University School of Medicine. At twelve weeks of age, wild type congenic and *rgs4*$^{-/-}$ C57/B6 mice were subjected to unilateral nephrectomy as previously described [28]. After a seven day recovery period, mice were administered a daily dose of intraperitoneal cyclosporine A (0.25 mg/g/day)[29],

or cyclosporine + bosentan for seven days. Intraperitoneal cyclosporine dose was determined by the smallest daily amount needed to achieve renal cortical vasoconstriction. Bosentan (Actelion Ltd, Switzerland) was administered through the animals' drinking water (2.35 mg/mL) to achieve a daily dose of 100 μg/g of body weight [30] based on an average urine output of 850 microliters per day.

Renal histology and morphometry

Mice were weighed, and kidneys isolated. Tissue was fixed in 10% formalin, paraffin-embedded, microtome sectioned and stained with hematoxylin and eosin (H&E). Tissue slices with maximum longitudinal dimension were used to estimate glomerular number. Separate slices were prepared and stained immunohistochemically with phospho-ERK 1/2 (Thr183/Tyr185) (Abcam Inc.; Cambridge, MA). Tissue cross-sectional areas from medulla of 4 mice were measured at low power (2.5x) and were calculated on an Axioskop microscope (Carl Zeiss, Inc., Jena, Germany) using ImageJ (version 1.24) software. Lean body mass was measured by EchoMRI 3-in-1 (Echo Medical Systems, Houston, TX) at 8 weeks after SIRI.

Gene expression analysis

Gene expression profiles were constructed using the GeneChip® Mouse Genome 430A 2.0 (Affymetrix, Southern Oaks, CA) high density olignouncleotide microarray technique. mRNA purification and analysis were performed by the Siteman Cancer Center GeneChip Facility as previously described[31]. Expression signaling was analyzed used Affymetrix Expression Console Software.

Quantitative real-time RT-PCR analysis on RNA extracted from kidney tissue lysates with Trizol reagent (Invitrogen Corp, Carlsbad, California) was carried out with the Taqman master mix kit (Applied Biosystems, Foster City, California) using RGS4 oligonulceotide primers (SABiosciences Corp., Frederick, MD) according to the manufacturer's specifications. The measured abundances of RGS4 mRNA were normalized to GAPDH in each sample as an internal loading control.

Protein analysis

Cytosolic protein lysates from kidney tissue were obtained as previously described[32]. In brief, tissue was harvested from mice, and lysates were processed in the presence of protein lysis buffer. Once processed, protein bound to nitrocellulose filters were washed and incubated with murine monoclonal anti-phospho-p44/42 (Thr202/Tyr204) and anti-total-p44/42 (Cell Signaling Technology, Inc., Beverly, MA). Bands were visualized by use of the ECL system (Amersham). Densitometry was performed using Image J software v1.24.

Vascular flow measurements

Transthoracic echocardiography and renal artery doppler sonography was performed in mice using a VEVO-770TTM Micro-Imaging System (Visual Sonic,Toronto, Ontario) equipped with a 15 MHz transducer. Prior to the imaging experiments, mice were anesthetized with isoflurane and were maintained on isoflurane/O_2 (1–1.25 % v/v) throughout data collection. The sonographer was blinded in all cases to the transgenic status of the mice. 10 consecutive waveforms were averaged to obtain a mean systolic velocity for each animal.

Renal artery blood velocity was measured using an Advanced Laser Flowmeter 21 (ALF21, ADVANCE Co., Tokyo, Japan). Mice were anesthetized with a mixture of xylazine (16 mg/kg) and ketamine (0.080 mg/g). A sham procedure was performed exposing the right kidney but maintaining its blood supply. The flow meter probe was applied directly to the renal artery and then to the hilum.

A volume pressure recording (VPR) device (Kent Scientific Corp., Torrington, CT) was used for tail cuff blood pressure measurements of mice at baseline. Mice were trained for two days immediately followed by measurements on day three. Mice were constrained in an adjustable plexiglass tube provided as a part of the VPR apparatus. A heating pad was placed under the tube to maintain a constant temperature between 31–33C°. Five training cycles were followed by five measurement cycles and then averaged.

Magnetic resonance imaging of renal blood flow in mice

MR images were collected using a dedicated small-animal MR scanner built around a 4.7 tesla, 40-cm bore magnet and interfaced with a Varian INOVA console. A home-built, actively decoupled volume coil (transmit)/surface coil (receive) pair were used for all image acquisitions. Prior to the imaging experiments, mice were anesthetized with isoflurane and were maintained on isoflurane/O_2 (1–1.25 % v/v) throughout data collection. Animal core-body temperature was maintained at 37 ±1 °C via a heating pad formed with circulating warm water. Dynamic contrast enhanced (DCE) MRI [33, 34] data were collected using a T1-weighted, gradient spoiled, multi-slice gradient-echo sequence. Further details of this procedure are found in the online supplemental data.

Quantitation of body fluid constituents

Levels of whole blood hemoglobin and serum blood urea nitrogen were measured in the Department of Comparative Medicine Diagnostic Laboratory at Washington University School of Medicine. Because of the imprecision of the Jaffe method in measuring mouse serum creatinine we collaborated with Satish Ramachandrarao at University of California, San Diego, California, to perform serum creatinine by HPLC as previously described [28, 35].

Cyclosporine trough levels were measured with the automated Dimension® RxL Max® clinical chemistry system from Siemens. Healthcare Diagnostics, Ltd. using an immunoassay technique. The assay was performed using a Flex ® reagent cartridge. Each sample of whole blood lysate was processed with the Dimension ® system platform.

Statistical analysis

All data are presented as mean values ± standard error of the mean. Static group analysis was performed with SigmaStat® 3.1 (Systat Software, Inc., San Jose, CA). Statistical relationships were determined by the student's T-test where significance was achieved when a population's mean value was separated from controls by two or more standard deviations ($p = 0.05$). All p-values calculated were two-sided. One-way ANOVA analysis was used in comparisons of greater than 2 groups, and Holm-Sidak pairwise comparisons were calculated between groups. Kaplan Meier survival curves and Mantel Cox log-rank analysis was performed with SPSS v13.0 (SPSS Inc., Chicago, IL). Pearson's correlation coefficient was performed on signal intensities generated from two separate gene expression microarrays. The Bootstrap algorithm for error estimation of gene expression microarray data [36] was performed using the Wessa.Net server version 1.1.23-r4.

Results

To generate mice deficient for RGS4 we created a genetic construct that eliminated exons 3–5 of the *rgs4* gene, encoding the RGS box (Suppl. Fig. 1). *Rgs4*$^{-/-}$ mice appeared normal at birth and were fertile. Mating of *rgs4*$^{+/-}$ heterozygotes yielded live-born homozygotes with Mendelian frequencies. Analysis of *rgs4*$^{-/-}$ mice in the absence of provocative stimulation demonstrated that these animals had comparable physiologic parameters. Normalized kidney weight was equal with no evidence of hypertension by noninvasive testing. These findings

were correlated with equivalent glomerular number. Renal function as estimated by serum creatinine was nearly identical in in *rgs4*$^{-/-}$ and wild type mice (0.106 ± 0.002 mg/dL vs 0.105 ± 0.007 mg/dL, p=0.89). (Suppl. Table 1). Normalized mRNA expression of RGS2, RGS5, RGS10, RGS12, and RGS16 was not increased in *rgs4*$^{-/-}$ mice (Suppl. Fig. 2a,b; Supplemental Table 2).

Calcineurin inhibitors are among the most commonly used immunomodulatory agents in transplantation, but they often cause marked renal dysfunction[18]. Specifically, cyclosporine A (CyA) causes acute renal injury due to decreased intrarenal blood flow [4, 25, 26]. Chronic injury mimics this mode of injury with histologic changes consistent with long term hypoxic injury described as striped fibrosis[37]. To determine whether *rgs4*$^{-/-}$ mice were sensitized to cyclosporine-mediated renal injury, we subjected animals to unilateral nephrectomy followed one week later by treatment with CyA. Congenic wild type control mice developed renal dysfunction within one week following CyA administration. By HPLC, serum creatinine increased 108% (0.2201 mg/dL vs. 0.106 mg/dL) (Fig. 1a) and BUN increased 274% (71 mg/dL) (Fig. 1b) in *rgs4*$^{-/-}$ mice versus controls after seven days of cyclosporine exposure while whole blood cyclosporine levels were equivalent between groups (Suppl. Fig. 3). Furthermore, there was no evidence that *rgs4*$^{-/-}$ mice metabolized cyclosporine less efficiently than congenic controls (Suppl. Fig. 4). Serum creatinine by HPLC approximates serum creatinine by the Jaffe method using a correction factor of 3.125. The Jaffe-equivalent measure in *rgs4*$^{-/-}$ given cyclosporine mice was 0.688 ± 0.044 mg/dL[35]. Disruption of the apical membrane of proximal tubular cells, indicative of acute tubular necrosis, was seen by light microscopy and electron microscopy (Fig. 2a,b). Renal artery blood flow to the kidney was decreased in cyclosporine-treated mice as measured by noninvasive Doppler sonography (Suppl. Fig. 5a,b), further implicating CyA exposure in the development of acute tubular necrosis. Noninvasive measurements could not differentiate the decrease in blood flow between *rgs4*$^{-/-}$ and controls, however, *rgs4*$^{-/-}$ mice had a decreased average renal artery flow velocity compared to congenic wild type control animals using invasive monitoring techniques (Suppl. Fig. 6). Smaller intrarenal vascular substructures could not be interrogated due to the limitations of current modalities of measuring *in vivo* renal blood flow.

To determine whether *rgs4*$^{-/-}$ mice developed more profound regional intrarenal vasoconstriction after CyA treatment, dynamic-contrast enhanced magnetic resonance imaging (DCE-MRI) [34, 38, 39] was used to quantitatively measure the uptake and clearance kinetics of a low molecular weight, Gadolinium-based MR contrast agent (CA). High-resolution, T1-weighted kidney images allowed clear visualization of the cortex, medulla, and renal pelvis together with accompanying intrarenal vasculature (Fig. 3). Selected images from the DCE time course and complete plots of adjusted signal intensity versus time allowed the CA kinetics to be accurately measured. A 42% decrease in blood flow was identified in the renal cortex (Fig. 4a, 5a). In contrast to congenic wild type controls, $IAUC_{60}$ decreased by 62% in the medulla of CyA-treated *rgs4*$^{-/-}$ mice, indicative of a significant decrease in regional blood flow (Fig. 4b, 5b). Blood flow was restored to both the medulla and the cortex with the coadministration of bosentan (**5a, 5b**). Cyclosporine's specific ability to activate an RGS-dependent signal transduction pathway is supported by the amelioration of its deleterious effect by administration of the endothelin receptor antagonist bosentan.

The ability of bosentan to reduce cyclosporine-mediated renal toxicity may be due to altered cyclosporine blood levels. To investigate this possibility, *rgs4*$^{-/-}$ mice were given escalating doses of cyclosporine with bosentan (100μg/g/d) (see Suppl. Fig. 7). Cyclosporine blood levels increased with higher doses of cyclosporine and were not affected by coadministration of bosentan.

Mice were next observed for a month while being treated with cyclosporine. *Rgs4*$^{-/-}$ mice exhibited significantly reduced survival in response to treatment with CyA when compared to congenic wild type control mice (Fig. 6). The mean survival time was 25 days for congenic wild type control mice in response to CyA administration, but *rgs4*$^{-/-}$ mice had a mean survival time of only 9 days (Mantel-Cox log rank test, p= 0.002). *rgs4*$^{-/-}$ mice coadministered cyclosporine and bosentan exhibited a significantly increased survival rate compared to *rgs4*$^{-/-}$ mice given cyclosporine alone.

CyA renal toxicity is thought to be due to the action of endothelin-1. Given the reduced intrarenal blood flow observed in CyA-treated *rgs4*$^{-/-}$ mice, we hypothesized that the absence of RGS4 protein would sensitize kidney to CyA- and endothelin-1-stimulated intracellular signal transduction. Sections of freshly obtained *rgs4*$^{-/-}$ and wild type congenic kidneys were treated in vitro with CyA or endothelin-1 for 10 minutes and processed for immunoblotting with an anti-phospho-ERK1/2 primary antibody. *rgs4*$^{-/-}$ kidney slices exhibited markedly increased ERK activation in response to endothelin-1 (Fig. 7a,c). Similarly, *rgs4*$^{-/-}$ kidney slices exposed to CyA for 10 minutes showed increased ERK activation (Fig. 7b,d). *In vivo* experiments demonstrated that ERK activation was increased in the kidneys of *rgs4*$^{-/-}$ mice treated with cyclosporine for 1 week (Fig. 8a,b). Interestingly, RGS4 mRNA levels rose by 1.75-fold in wild type congenic kidneys after 7 days of CyA treatment (Fig 8c).

Rgs4$^{-/-}$ kidneys were sensitized to CyA-mediated reduction in renal blood flow and were also sensitized to endothelin-1 mediated ERK activation. Given that CyA-mediated acute renal toxicity correlates with increased endothelin-1 release, and that bosentan is a widely used ET-A/B receptor antagonist, mice were treated with this agent. Administration of bosentan to *rgs4*$^{-/-}$ mice abrogated the effect of CyA on blood perfusion in the kidney (Fig. 4a, 4b, 5a, 5b) and ERK phosphorylation decreased to pre-cyclosporine levels in bosentan-treated animals (Fig. 8a,b).

Discussion

Calcineurin inhibitors are the most commonly used immunosuppressive agents in the prevention of solid organ transplant rejection [17], but cause progressive renal toxicity [40, 41]. CNI nephrotoxicity is in part due to endothelin-1 release by vascular endothelial cells promoting renal vasoconstriction and reduction in renal blood flow. The mechanism by which cyclosporine causes endothelin-1 release is unclear. Although cyclosporine directly binds to L-type calcium channels *in vitro* [42], the secondary release of endothelin-1 stimulates Gq signaling that results in inositol triphosphate binding to L-type calcium channels [43]. Therefore the direct link between calcineurin inhibition and elevated sarcoplasmic calcium levels is contested [44]. However, after endothelin-1 is released acutely, cyclosporine initiates a maintenance phase of endothelin release and upregulation of endothelin gene expression. Marsen and colleagues determined that both cyclosporine and tacrolimus promote the transcription of preproendothelin-1 mRNA in human vascular endothelial cells [45].

In this work, we described for the first time, the *in vivo* vasoactive effects of cyclosporine A in a minimally invasive mouse model. Because the compact size of the mouse model system is more difficult to analyze than larger mammals, innovative methods are needed to analyze mouse renal and renovascular physiology in a reproducible manner. These adaptations are vital for the translation of animal studies to human therapy.

We hypothesized that RGS4 plays a key role in regulating renal vascular resistance through modulation of Gq activation. We found that *rgs4*$^{-/-}$ mice were uniquely susceptible to a

reduction in renal medullary blood flow mediated by cyclosporine. Previous studies by Lee et al, Mazzali et al, and Neria et al [29, 46, 47] could not demonstrate an increase in serum creatinine after exposure to cyclosporine and therefore relied predominantly on histologic markers of renal injury. In this study, we showed that *rgs4*$^{-/-}$ mice had a 108% increase in serum creatinine and 274% increase in BUN compared to congenic controls after both groups were exposed to cyclosporine for one week. These results link RGS4 deficiency and a susceptibility to renal failure.

The specificity of cyclosporine's action through the G-protein signaling cascade was demonstrated when bosentan, an endothelin A/B receptor antagonist, prevented the deleterious effect of cyclosporine on renal function. We also found that endothelin-1-mediated activation of ERK was enhanced in *rgs4*$^{-/-}$ kidney. This result follows the previous findings of Albig et al who showed that *in vitro* overexpression of RGS4 prevented ERK activation in the presence of endothelin- 1[27]. These results establish that RGS4 is a key regulator of endothelin-1 action in the kidney, probably via effects on Gq.

The use of bosentan in transplantation is relatively contraindicated because of increased hypotension when coadministered with cyclosporine A. Only one human study to date by Binet et al has evaluated the renal hemodynamic effects of endothelin receptor antagonists on calcineurin inhibitors [48]. Binet et al reported a mean systolic/diastolic blood pressure of 135 ± 6 / 80± 4 mmHg in seven patients given cyclosporine A alone which was comparable to internal controls given cyclosporine A and bosentan (136 ± 8/ 80± 7 mmHg). Limited animal studies remain unclear [49, 50]. Further studies are needed to delineate the potentional hypotensive effects of calcineurin inhibitors when used in combination with endothelin receptor antagonists.

Our MRI results showed that CyA-treated *rgs4*$^{-/-}$ kidneys exhibited a greater decrease in signal intensity in the renal medulla than in the renal cortex, suggesting that RGS4 modulates vasoconstriction proximal to the vascular network of the medulla. Studies of CyA thus far have investigated the ligands responsible for initiating the intracellular signaling cascade that leads to smooth muscle vasoconstriction in the kidney [49, 51–54]. Lanese and colleagues were the first to show that cyclosporine was specific to the endothelin ligand [4]. In our current study we describe a specific intracellular pathway that is activated by cyclosporine, and directs future studies to targeted inhibition of the G-protein signaling system or promotion of the inhibitory activities of RGS4.

To study the vasoconstrictive properties of cyclosporine we used a novel DCE-MRI, and were able to describe, in detail, contrast-agent uptake and clearance kinetics in the mouse kidney. Our studies focused on monitoring the regionalized effects of CyA treatment. These observed changes in CA kinetics following treatment with CyA reflect physiologic changes in the kidney that are consistent with a stepwise reduction of renal blood flow in the cortex and the medulla. While microbead radioisotope methods remain the gold standard for measuring end-organ perfusion [55, 56], these methods can not be applied *in vivo*. Measuring alteration of organ blood flow with microbeads is limited by the need for post mortem tissue preparation. MR methods are non-invasive, enabling longitudinal, time-course studies of blood-flow patterns in response to interventions.

Conclusion

The large number of RGS family members implies that there is specific requirement for particular members in various cell types and organ systems. The role of RGS proteins in the management of renal vascular insult is not well understood. In this work, we demonstrated that RGS4 plays a specific role in modulating renal insults that occur as a consequence of

overstimulation of the Gq signaling pathway. Increasing RGS4 protein levels by inhibiting proteasomal degradation or increasing activity through in the kidney may be therapeutically beneficial for patients with renal dysfunction.

Supplementary Material

Refer to Web version on PubMed Central for supplementary material.

Acknowledgments

The authors had full access to the data and take responsibility for its integrity. All authors have read and agree to the manuscript as written. We acknowledge Dr. Joseph J.H. Ackerman for the generous contribution of his time spent on the conceptual design of this project. This work was supported by NIH grants RO1 HL061567, RO1 HL076670, and P01 HL057278 (A.J.M.). We thank the Alvin J. Siteman Cancer Center at Washington University School of Medicine and Barnes-Jewish Hospital in St. Louis, Mo., for use of the Center for Biomedical Informatics and Multiplex Gene Analysis Genechip Core Facility. The Siteman Cancer Center is supported in part by a NCI Cancer Center Support Grant #P30 CA91842. A portion of this data was presented at the 2009 American Transplant Congress, abstract 1703.

Fundings Sources: This work was supported by the Mallinckrodt Institute of Radiology and by NIH grants RO1 HL061567 (A.J.M.), P01 HL057278 (A.J.M.), RO1 HL 076670 (A.J.M.), and P30 DK079333 (A.S., A.J.M.), and U24 CA83060 (J.G., J. J. H. A.).

References

1. Pallone TL, Silldorff EP, Turner MR. Intrarenal blood flow: microvascular anatomy and the regulation of medullary perfusion. Clin Exp Pharmacol Physiol. 1998; 25:383–392. [PubMed: 9673811]
2. Arendshorst WJ, Brannstrom K, Ruan X. Actions of angiotensin II on the renal microvasculature. J Am Soc Nephrol. 1999; 10:S149–S161. [PubMed: 9892156]
3. Naicker S, Bhoola K. Endothelins: vasoactive modulators of renal function in health and disease. Pharmacol Ther. 2001; 90:61–88. [PubMed: 11448726]
4. Lanese DM, Conger J. Effects of endothelin receptor antagonist on cyclosporine-induced vasoconstriction in isolated rat renal arterioles. J Clin Invest. 1993; 91(5):2144–2149. [PubMed: 8486781]
5. Lefkowitz R. Seven transmembrane receptors: something old, something new. Acta Physiol. 2007; 190:9–19.
6. Wilson BA, Zhu X, Ho M, Lu L. Pasteurella multocida toxin activates the inositol triphosphate signaling pathway in Xenopus oocytes via G(q)alpha-coupled phospholipase C-beta1. J Biol Chem. 1997; 272(2):1268–1275. [PubMed: 8995431]
7. Sternweis PC, Smrcka A. G proteins in signal transduction: the regulation of phospholipase C. Ciba Found Symp. 1993; 176:96–106. [PubMed: 8299429]
8. Ratz PH. Regulation of ERK phosphorylation in differentiated arterial muscle of rabbits. Am J Physiol Heart Circ Physiol. 2001; 281(1):H114–H123. [PubMed: 11406475]
9. Ishida M, Ishida T, Thomas SM, Berk BC. Activation of extracellular signal-regulated kinases (ERK1/2) by angiotensin II is dependent on c-Src in vascular smooth muscle cells. Circ Res. 1998; 82(1):7–12. [PubMed: 9440699]
10. Adam LP, Franklin MT, Raff GJ, Hathaway DR. Activation of mitogen-activated protein kinase in porcine carotid arteries. Circ Res. 1995; 76(2):183–190. [PubMed: 7834828]
11. Dikic I, Tokiwa G, Lev S, Courtneidge SA, Schlessinger J. A role for Pyk2 and Src in linking G-protein-coupled receptors with MAP kinase activation. Nature. 1996; 383(6600):547–550. [PubMed: 8849729]
12. Touyz RM, He G, Deng LY, Schiffrin EL. Role of extracellular signal-regulated kinases in angiotensin II-stimulated contraction of smooth muscle cells from human resistance arteries. Circulation. 1999; 99(3):392–329. [PubMed: 9918526]

13. Berman DM, Wilkie T, Gilman AG. GAIP and RGS4 are GTPase-activating proteins for the Gi subfamily of G protein alpha subunits. Cell. 1996; 86(3):445–452. [PubMed: 8756726]
14. Bansal G, Druey KM, Xie Z. R4 RGS proteins: regulation of G-protein signaling and beyond. Pharmacol Ther. 2007; 116(3):473–495. [PubMed: 18006065]
15. Higgins JP, Wang L, Kambham N, Montgomery K, Mason V, Vogelmann SU. Gene expression in the normal adult human kidney assessed by complementary DNA microarray. Mol Biol Cell. 2004; 15(2):649–656. [PubMed: 14657249]
16. Bodenstein J, Sunahara R, Neubig RR. N-terminal residues control proteasomal degradation of RGS2, RGS4, and RGS5 in human embryonic kidney 293 cells. Mol Pharmacol. 2007; 71(4): 1040–1050. [PubMed: 17220356]
17. Meier-Kriesche HU, Li S, Gruessner RW, Fung JJ, Bustami RT, Barr ML, et al. Immunosuppression: evolution in practice and trends, 1994–2004. Am J Transplant. 2006; 6(5): 1111–1131. [PubMed: 16613591]
18. Olyaei AJ, de Mattos A, Bennett WM. Nephrotoxicity of immunosuppressive drugs: new insight and preventive strategies. Curr Opin Crit Care. 2001; 7(6):384–389. [PubMed: 11805539]
19. Naesens M, Kuypers DR, Sarwal M. Calcineurin inhibitor nephrotoxicity. Clin J Am Soc Nephrol. 2009; 4(2):481–508. [PubMed: 19218475]
20. Krysztopik RJ, Bentley FR, Spain DA, Wilson MA, Garrison RN. Lazaroids prevent acute cyclosporine-induced renal vasoconstriction. Transplantation. 1997; 63(9):1215–1220. [PubMed: 9158012]
21. Rezzani R. Exploring cyclosporine A-side effects and the protective role-played by antioxidants: the morphological and immunohistochemical studies. Histol Histopathol. 2006; 21(3):301–316. [PubMed: 16372251]
22. Bobadilla NA, Gamba G. New insights into the pathophysiology of cyclosporine nephrotoxicity: a role of aldosterone. Am J Physiol Renal Physiol. 2007; 293(1):F2–F9. [PubMed: 17429034]
23. Ramzy D, Rao V, Tumiati LC, Xu N, Miriuka S, Delgado D, Ross HJ. Role of endothelin-1 and nitric oxide bioavailability in transplant-related vascular injury: comparative effects of rapamycin and cyclosporine. Circulation. 2006; 114(1 Suppl):I214–I219. [PubMed: 16820575]
24. Gabriëls G, August C, Grisk O, Steinmetz M, Kosch M, Rahn KH, et al. Impact of renal transplantation on small vessel reactivity. Transplantation. 2003; 75(5):689–697. [PubMed: 12640311]
25. Perico N, Dadan J, Remuzzi G. Endothelin mediates the renal vasoconstriction induced by cyclosporine in the rat. J Am Soc Nephrol. 1990; 1(1)
26. Kon V, Sugiura M, Inagami T, Harvie BR, Ichikawa I, Hoover RL. Role of endothelin in cyclosporine-induced glomerular dysfunction. Kidney Int. 1990; 37(6):1487–1491. [PubMed: 2194067]
27. Albig AR, Schiemann W. Identification and characterization of regulator of G protein signaling 4 (RGS4) as a novel inhibitor of tubulogenesis: RGS4 inhibits mitogen-activated protein kinases and vascular endothelial growth factor signaling. Mol Biol Cell. 2005; 16(2):609–625. [PubMed: 15548600]
28. Siedlecki AM, Jin X, Muslin AJ. Uremic cardiac hypertrophy is reversed by rapamycin but not by lowering of blood pressure. Kidney Int. 2009; 75(8):800–808. [PubMed: 19165175]
29. Neria F, Castilla MA, Sanchez RF, Gonzalez Pacheco FR, Deudero JJ, et al. Inhibition of JAK2 protects renal endothelial and epithelial cells from oxidative stress and cyclosporin A toxicity. Kidney Int. 2009; 75(2):227–234. [PubMed: 18818682]
30. Sabaa N, de Franceschi L, Bonnin P, Castier Y, Malpeli G, Debbabi H, et al. Endothelin receptor antagonism prevents hypoxia-induced mortality and morbidity in a mouse model of sickle-cell disease. Clin Invest. 2008; 118(5):1924–1933.
31. Mahadevappa M, Warrington J. A high-density probe array sample preparation method using 10- to 100-fold fewer cells. Nat Biotechnol. 1999; 17(11):1134–1136. [PubMed: 10545926]
32. DeBosch B, Treskov I, Lupu TS, Weinheimer C, Kovacs A, Courtois M, et al. Akt1 is required for physiological cardiac growth. Circulation. 2006; 113(17):2097–2104. [PubMed: 16636172]

33. Knopp MV, Giesel F, Marcos H, von Tengg-Kobligk H, Choyke P, et al. Dynamic contrast-enhanced magnetic resonance imaging in oncology. Top Magn Reson Imaging. 2001; 12(4):301–308. [PubMed: 11687716]
34. Tofts PS, Brix G, Buckley DL, Evelhoch JL, Henderson E, Knopp MV. Estimating kinetic parameters from dynamic contrast-enhanced T(1)-weighted MRI of a diffusable tracer: standardized quantities and symbols. J Magn Reson Imaging. 1999; 10(3):223–232. [PubMed: 10508281]
35. Dunn SR, Qi Z, Bottinger EP, Breyer MD, Sharma K. Utility of endogenous creatinine clearance as a measure of renal function in mice. Kidney Int. 2004; 65(5):1959–1967. [PubMed: 15086941]
36. Brody JP, Williams BA, Wold BJ, Quake SR. Significance and statistical errors in the analysis of DNA microarray data. Proc Natl Acad Sci U S A. 2002; 99(20):12975–12978. [PubMed: 12235357]
37. Myers BD, Ross J, Newton L, Luetscher J, Perlroth M. Cyclosporine-associated chronic nephropathy. N Engl J Med. 1984; 311(11):699–705. [PubMed: 6382005]
38. Garbow JR, Mcintosh C, Conradi MS. Actively Decoupled Transmit-Receive Coil-Pair for Mouse Brain MRI. Concepts in Magnetic Resonance. 2008; 33:252–259.
39. Evelhoch JL. Key factors in the acquisition of contrast kinetic data for oncology. J Magn Reson Imaging. 1999; 10(3):254–259. [PubMed: 10508284]
40. Nankivell BJ, Borrows R, Fung CL, O'Connell PJ, Chapman JR, Allen RD. Calcineurin inhibitor nephrotoxicity: longitudinal assessment by protocol histology. Transplantation. 2004; 78(4):557–565. [PubMed: 15446315]
41. European multicentre trial of cyclosporine in renal transplantation: 10-year follow-up. Transplant Proc. 25(1):527–529. [PubMed: 8438401]
42. Schuhmann K, Romanin C, Baumgartner W, Groschner K. Intracellular Ca2+ inhibits smooth muscle L-type Ca2+ channels by activation of protein phosphatase type 2B and by direct interaction with the channel. J Gen Physiol. 1997; 110(5):503–513. [PubMed: 9348323]
43. Takuwa Y, Kasuya Y, Takuwa N, Kudo M, Yanagisawa M, Goto K. Endothelin receptor is coupled to phospholipase C via a pertussis toxinin-sensitive guanine nucleotide-binding regulatory protein in vascular smooth muscle cells. J Clin Invest. 1990; 85(3):653–658. [PubMed: 2155922]
44. Lo Russo A, Passaquin A, André P, Skutella M, Rüegg UT, et al. Effect of cyclosporin A and analogues on cytosolic calcium and vasoconstriction: possible lack of relationship to immunosuppressive activity. Br J Pharmacol. 1996; 118(4):885–892. [PubMed: 8799558]
45. Marsen TA, Weber F, Egink G, Suckau G, Baldamus CA. Differential transcriptional regulation of endothelin-1 by immunosuppressants FK506 and cyclosporin A. Fundam Clin Pharmacol. 2000; 14(4):401–408. [PubMed: 11030448]
46. Lee S, Kim W, Kim DH, Moon SO, Jung YJ, Lee AS, et al. Protective effect of COMP-angiopoietin-1 on cyclosporine-induced renal injury in mice. Nephrol Dial Transplant. 2008; 23(9):2784–2794. [PubMed: 18463324]
47. Mazzali M, Hughes J, Dantas M, Liaw L, Steitz S, Alpers CE, et al. Effects of cyclosporine in osteopontin null mice. Kidney Int. 2002; 62(1):78–85. [PubMed: 12081566]
48. Binet I, Wallnofer A, Weber C, Jones R, Thiel G. Renal hemodynamics and pharmacokinetics of bosentan with and without cyclosporine A. Kidney International. 2000; 57(1):224–231. [PubMed: 10620203]
49. Prévot A, Semama D, Tendron A, Justrabo E, Guignard JP, Gouyon JB. Endothelin, angiotensin II and adenosine in acute cyclosporine A nephrotoxicity. Pediatr Nephrol. 2000; 14(10–11):927–934. [PubMed: 10975301]
50. Soydan G, Tekes E, Tuncer M. Short-term and long-term FK506 treatment alters the vascular reactivity of renal and mesenteric vascular beds. J Pharmacol Sci. 2006; 102(4):359–367. [PubMed: 17130675]
51. Binet I, Wallnofer A, Weber C, Jones R, Thiel G. Renal hemodynamics and pharmacokinetics of bosentan with and without cyclosporine A. Kidney Int. 2000; 57(1):224–231. [PubMed: 10620203]
52. Bobadilla NA, Gamba G. New insights into the pathophysiology of cyclosporine nephrotoxicity: a role of aldosterone. Am J Physiol Renal Physiol. 2007; 293(1):2–9.

53. Perez-Rojas JM, Derive S, Blanco JA, Cruz C, Martinez de la Maza L, Gamba G, et al. Renocortical mRNA expression of vasoactive factors during spironolactone protectie effect in chronic cyclosporine nephrotoxicity. Am J Physiol Renal Physiol. 2005; 289(5):1020–1030.

54. Padi SS, Chopra K. Selective angiotensin II type 1 receptor blockade ameliorates cyclosporine nephrotoxicity. Pharmacol Ther. 2002; 45(5):413–420.

55. Sabto J, Bankir L, Grünfeld JP. The measurement of glomerular blood flow in the rat kidney: influence of microsphere size. Clin Exp Pharmacol Physiol. 1978; 5(6):559–565. [PubMed: 719956]

56. Ofstad J, Morkrid L, Willassen Y. Diameter of the afferent arteriole in the dog kidney estimated by the microsphere method. Scand J Clin Lab Invest. 1975; 35(8):767–774. [PubMed: 1209163]

1a

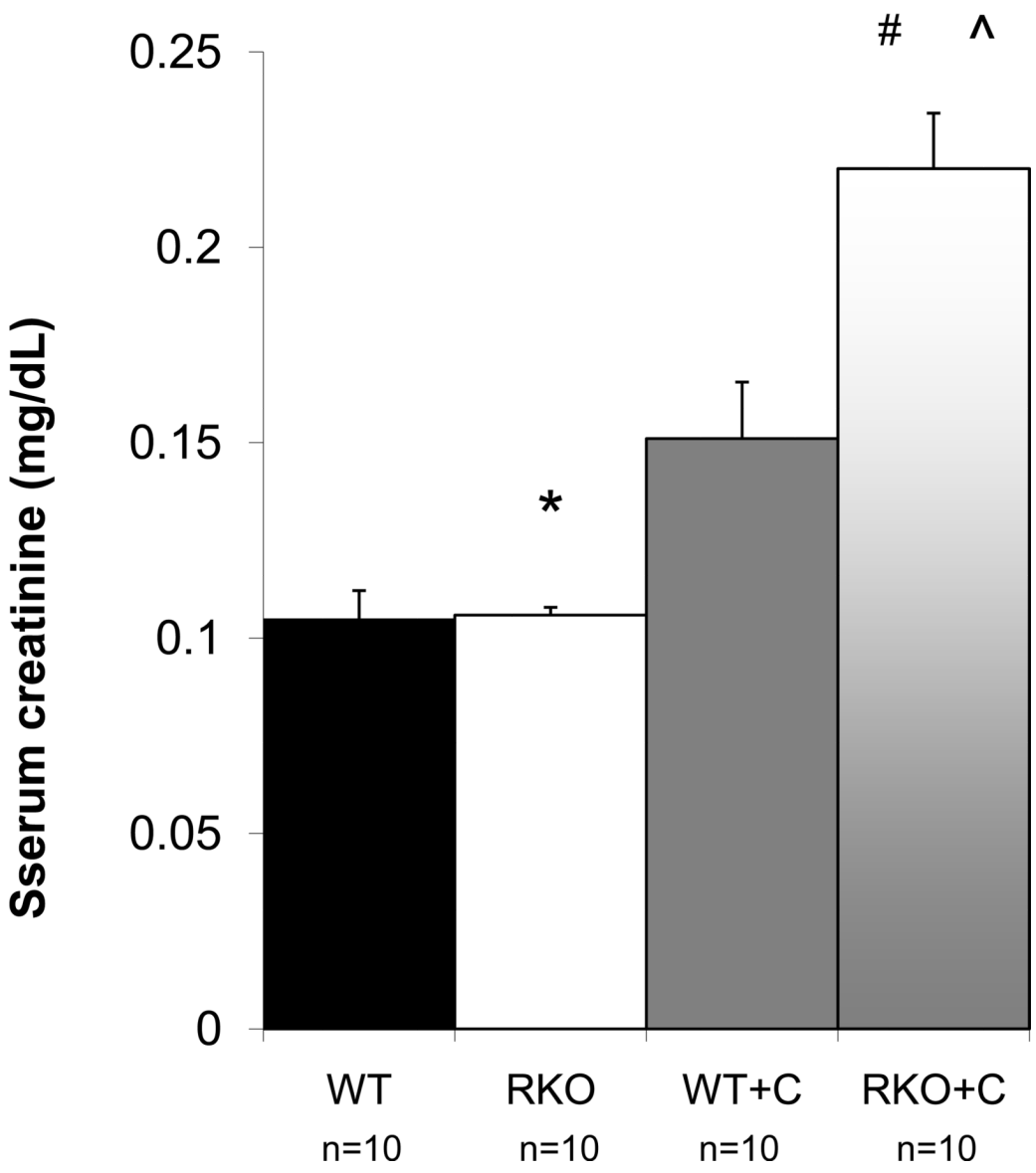

1b

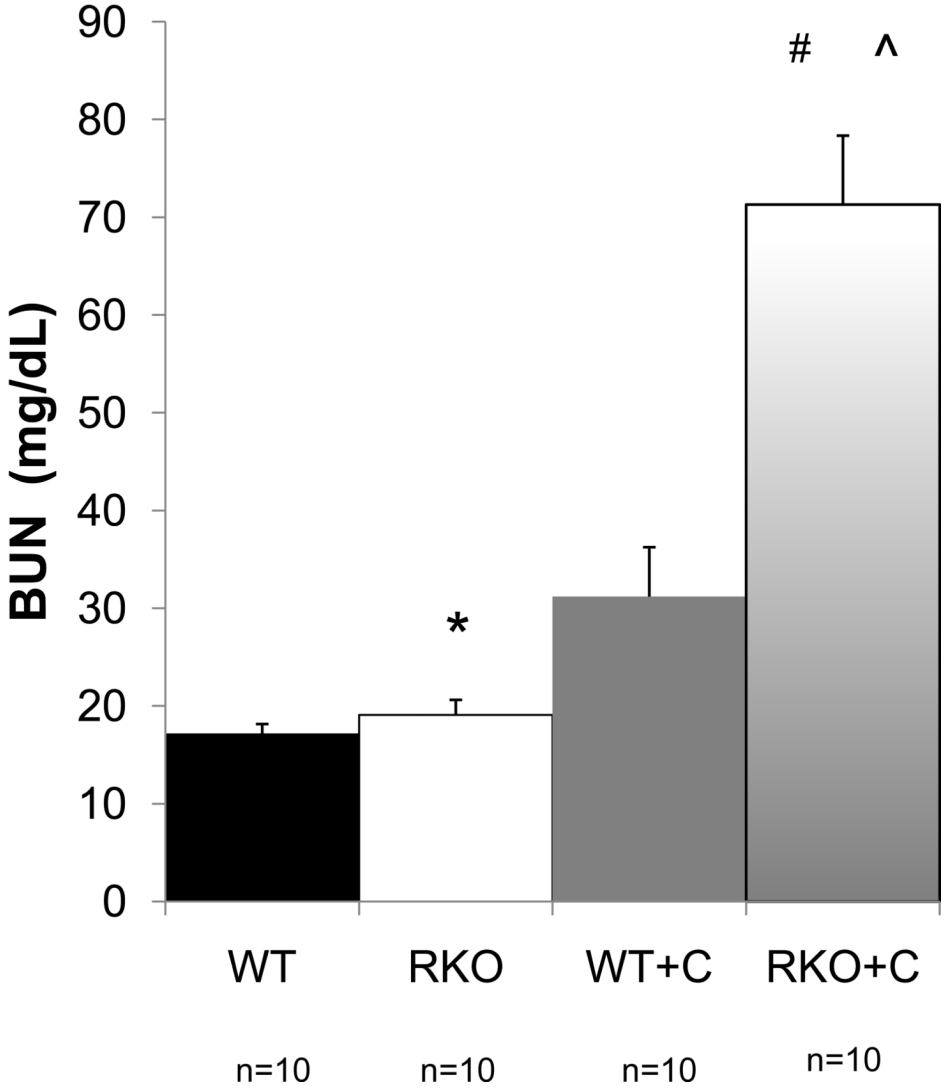

Figure 1.

Increased renal injury in *rgs4*$^{-/-}$ mice treated with cyclosporine A. After seven days of treatment with cyclosporine, (**a**) serum creatinine (sCr) was measured in *rgs4*$^{-/-}$ (RKO+C) (n=10) and wild type congenic mice (WT+C) (n=10). SCr was increased in RKO+C compared to other groups by one-way independent ANOVA: F(3,31) = 43.88, composite p <0.001; WT vs RKO = ***** (p = 0.89); RKO vs RKO+C = **#** (p=<0.0001); WT+C vs RKO+C = **^** (p<0.0001), (**b**) Blood urea nitrogen (BUN) was increased in RKO+C (n=10) compared to other groups by one-way independent ANOVA: F(3,35) = 31.12, composite p <0.0001; WT vs RKO = ***** (p = 0.89); RKO vs RKO+C = **#** (p=<0.0001); WT+C vs RKO+C = **^** (p<0.0001)

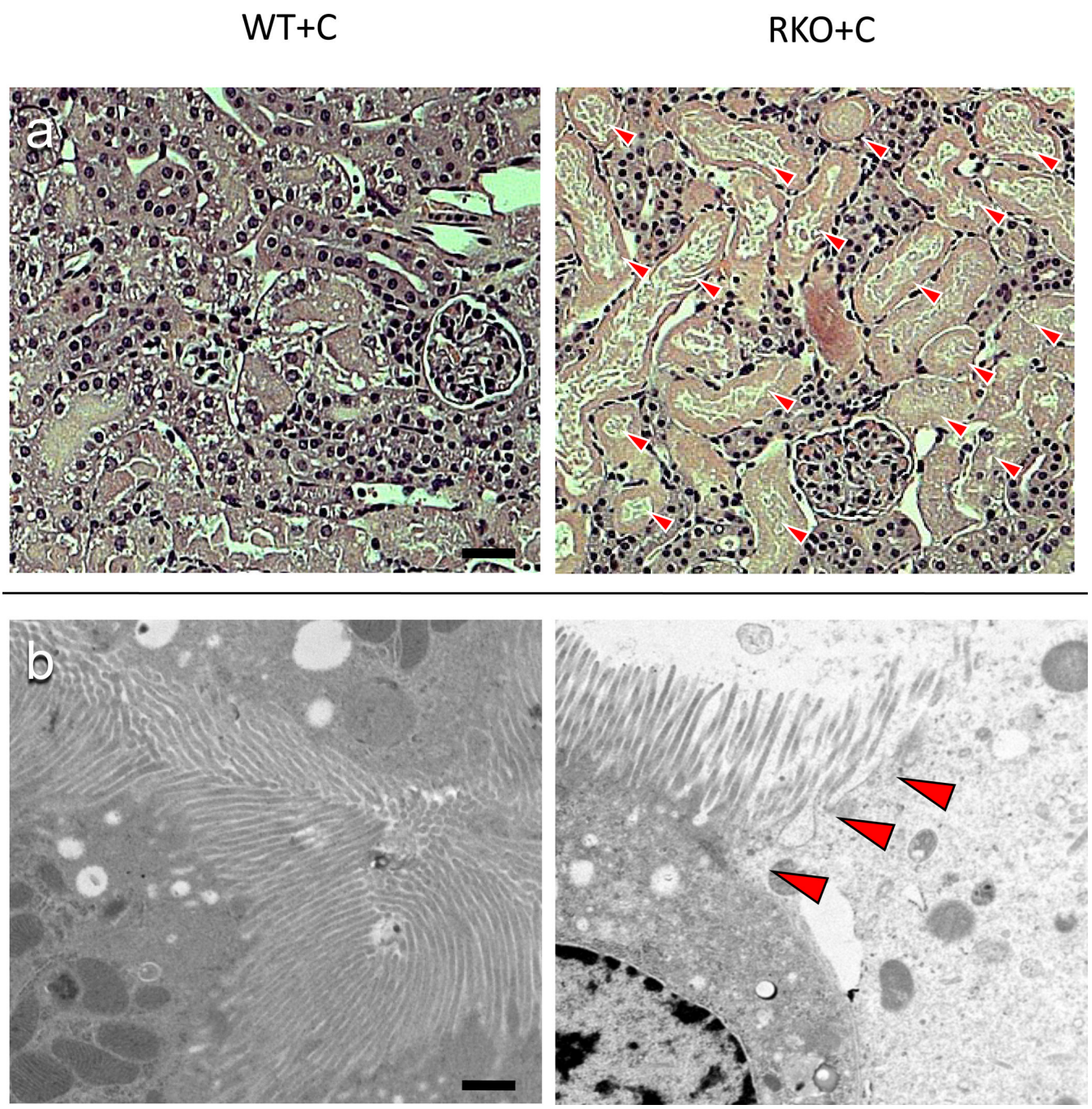

Figure 2.
Light and electron microscopy of congenic wild type + cyclosporine (WT+C) (n=4) and *rgs4*$^{-/-}$ + cyclosporine(RKO+C) (n=4).(**a**) The lumenal membrane of proximal tubule cells is disrupted and intralumenal debris is present in RKO+C (arrows) (magnification 400×). Scale bar = 200 micron. (**b**) The ciliary brush border on the apical membrane of epithelial proximal tubule cells (arrows) is also disrupted in RKO+C mice (n=4) compared to WT+C (n=4) (magnification 7500×). Scale bar = 2 microns.

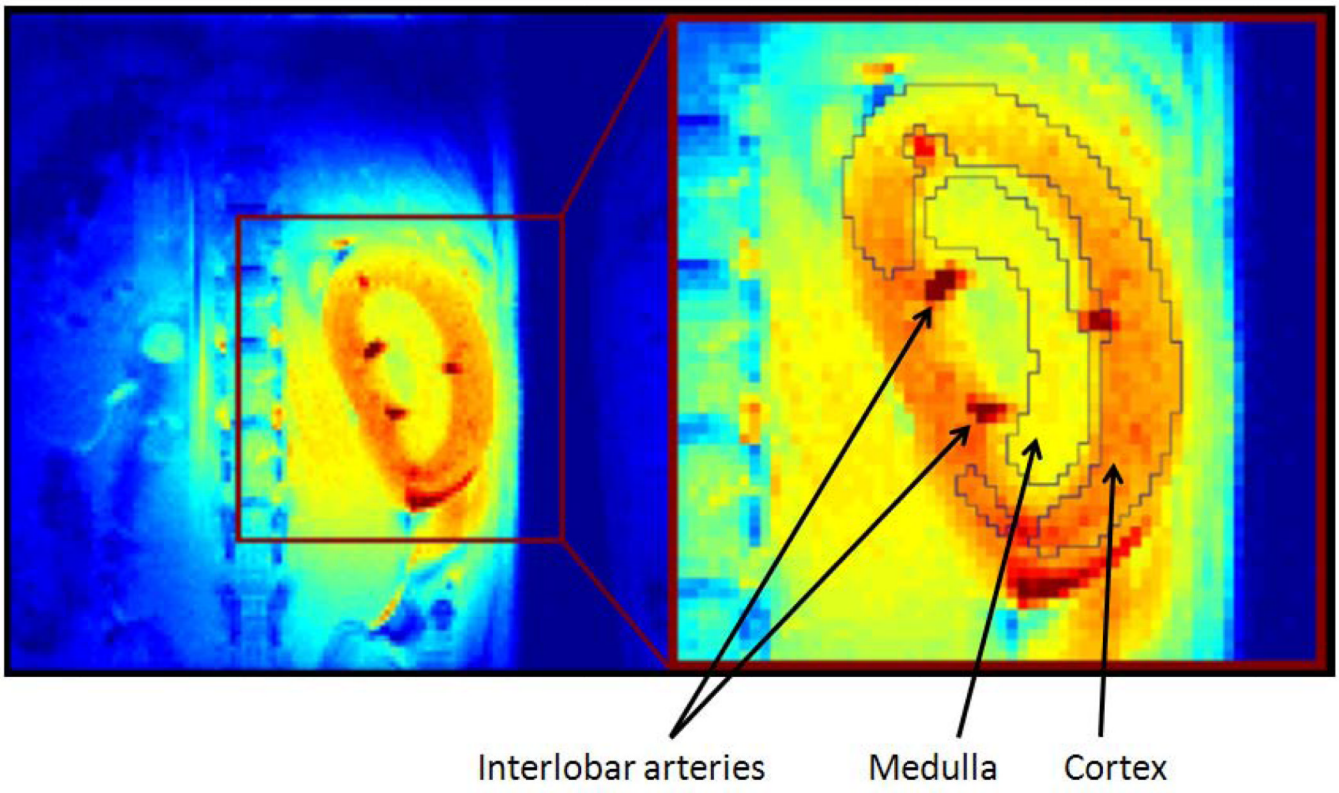

Figure 3.
High-resolution, T1-weighted image of a kidney from an *rgs4*$^{-/-}$ mouse, allowing clear visualization of the cortex, medulla, and renal pelvis and the intrarenal vasculature (intense red pixels).

4a

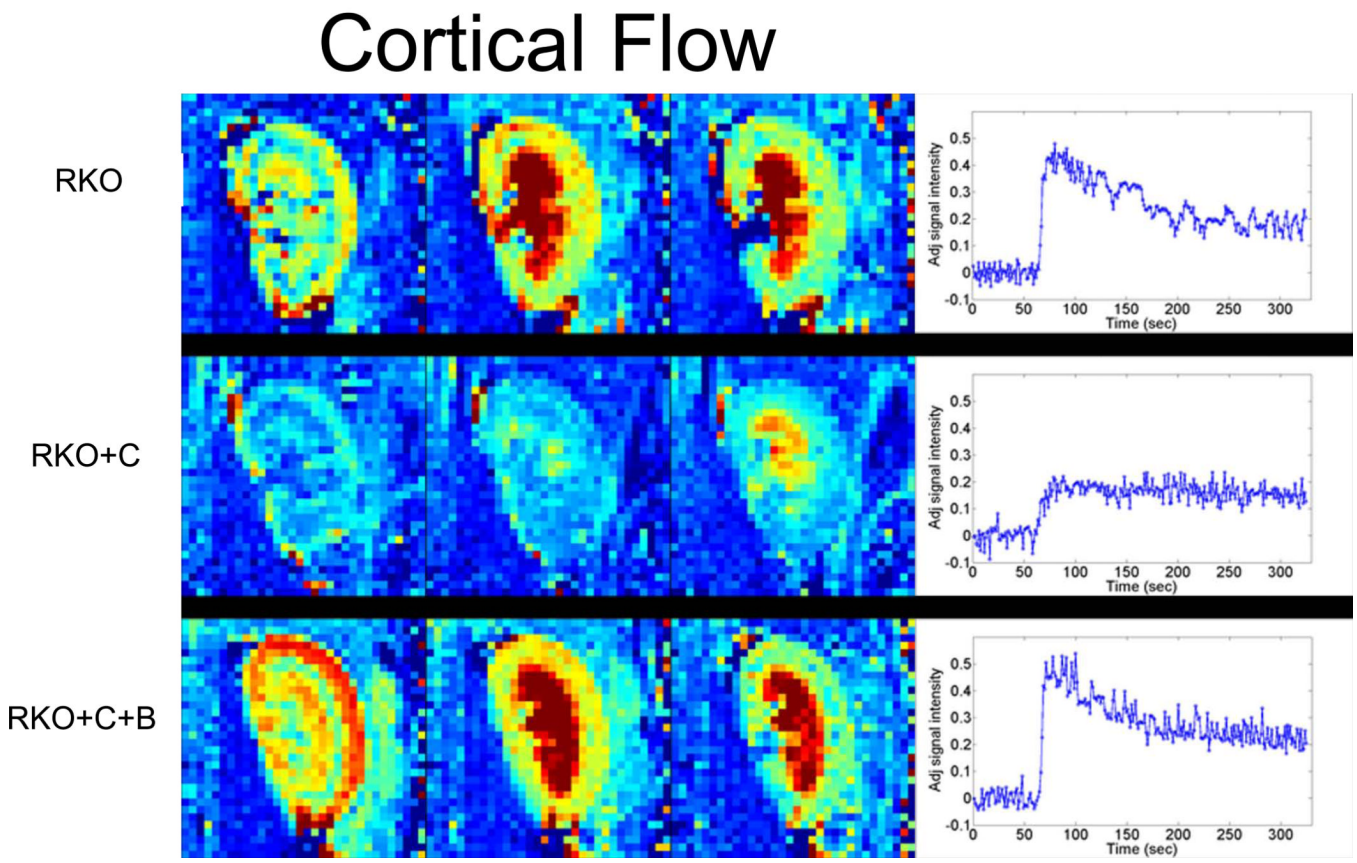

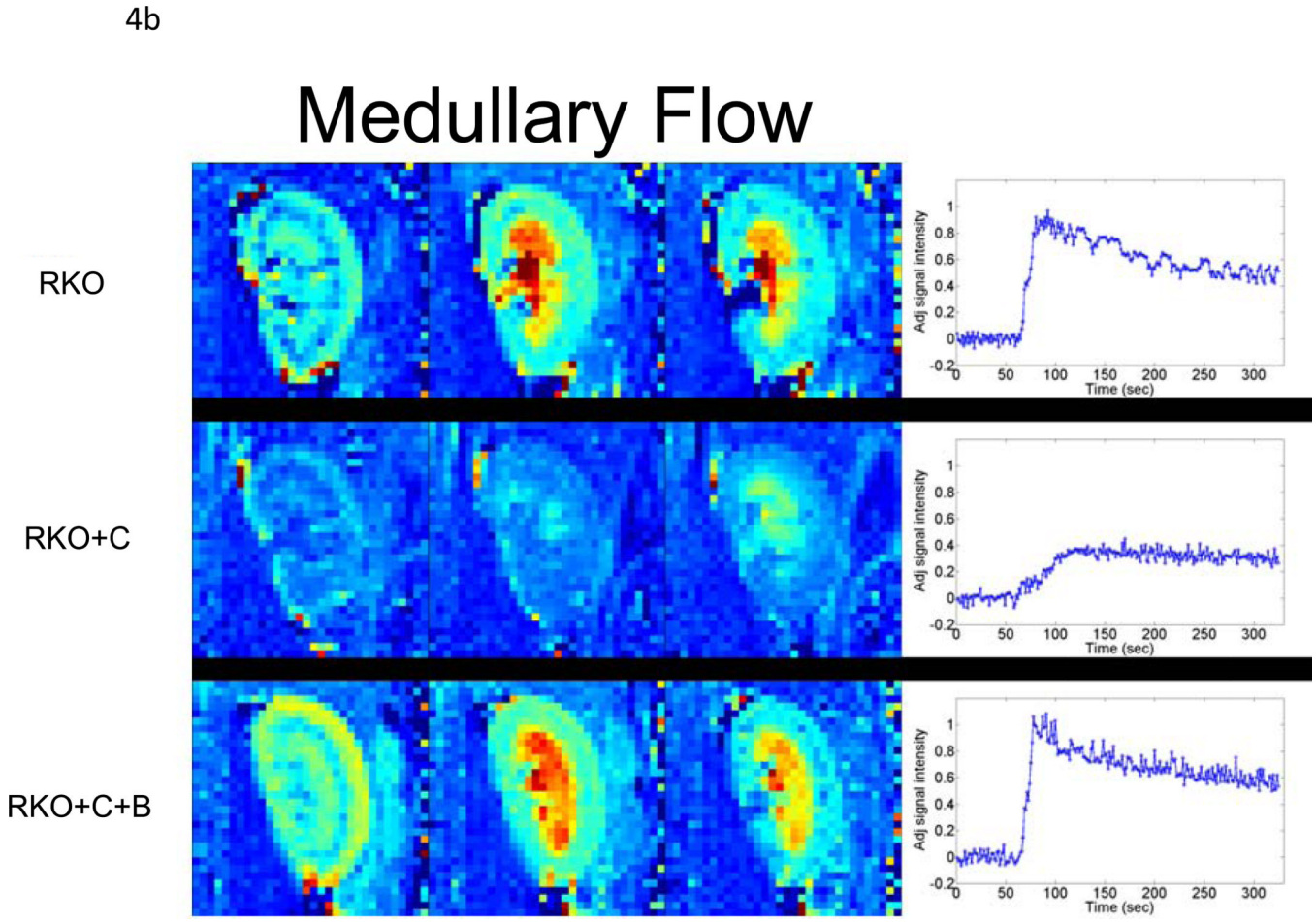

Figure 4.

Dynamic-contrast enhanced magnetic resonance imaging (DCE-MRI) data collected following bolus injection of a low molecular weight, Gd-containing contrast agent (adjusted signal intensity). Selected images from the (**a**) cortical and (**b**) medullary regions of interest are shown for: (top) a *rgs4*$^{-/-}$ mouse(RKO); (middle) a *rgs4*$^{-/-}$ mouse treated with Cyclosporine (RKO+C); (bottom) and a *rgs4*$^{-/-}$ mouse treated with Cyclosporine and bosentan (RKO+C+B). Images were collected 12 s (left panel), 38 s (middle panel) and 90 s (right panel) post-contrast injection. At the right, in each panel are the complete adjusted signal intensity vs. time curves for a (**a**) cortical ROI and (**b**) medullary ROI for each of these mice.

5a

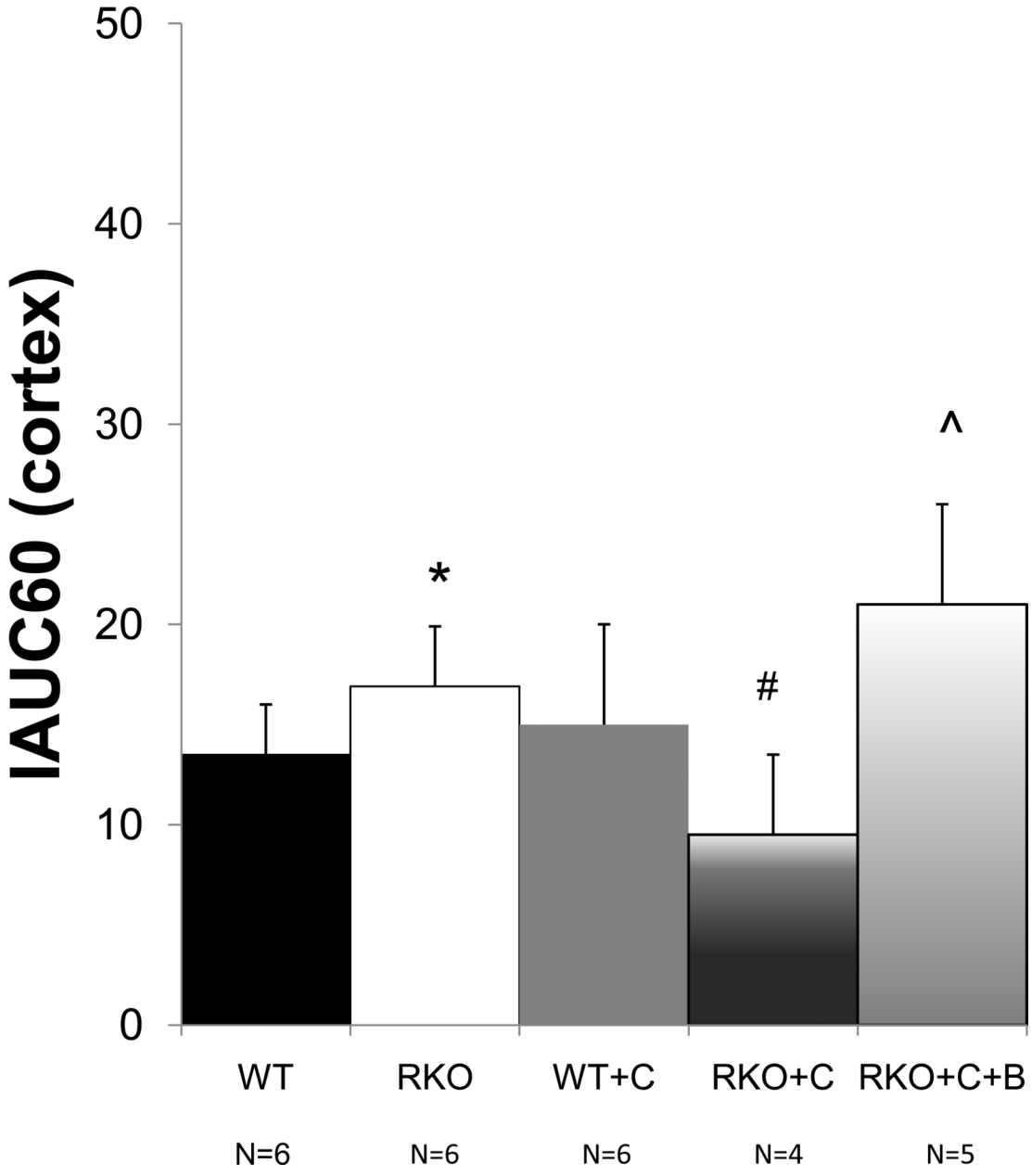

5b

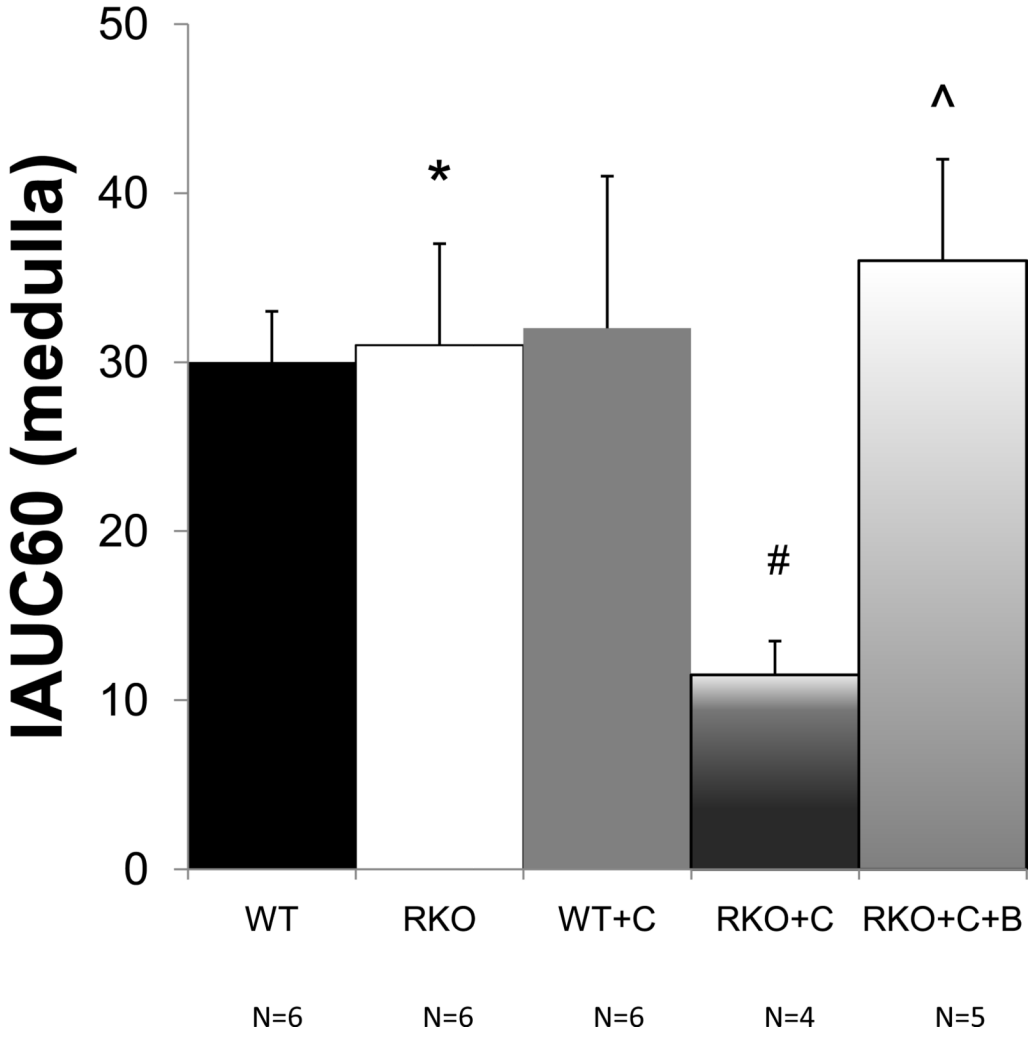

Figure 5.

Average initial area under the curve ($IAUC_{60}$) values, computed for the (**a**) cortical cohorts of wild-type (WT) (n=6), *rgs4*$^{-/-}$ (n=6), Cyclosporine-treated wild-type (WT+C) (n=6), cyclosporine-treated *rgs4*$^{-/-}$ (n=4), and *rgs4*$^{-/-}$ + cyclosporine + bosentan mice (n=5). Decreased rate of agent uptake in the cortex was evident in RKO+C by one-way independent ANOVA, F(3,61.7) = 5.5 (composite p=0.009). Blood flow was then restored with bosentan cotreatment comparing RGS4KO + cyclosporine + bosentan (RKO+C+B) to WT, RKO, and WT+C (One-way independent ANOVA, F(4,21) = 5.48 (composite p=0.003). WT vs. RKO, p = 0.79, * ; RKO vs RKO+C, p = 0.01, # ; RKO vs RKO +C+B, p=0.10, ^. (**b**) Medullary cohorts of wild-type (WT) (n=6), *rgs4*$^{-/-}$ (n=6), Cyclosporine-treated wild-type (WT+C) (n=6), cyclosporine-treated *rgs4*$^{-/-}$ (n=4), and *rgs4*$^{-/-}$ + cyclosporine + bosentan mice (n=5), showed a greater decrease in renal medullary blood

flow than cortical blood flow in *rgs4*$^{-/-}$ mice after cyclosporine treatment (RKO+C). (One-way independent ANOVA, $F(4,21) = 13.2.0$ (composite $p<0.0001$). Medullary blood flow was restored when *rgs4*$^{-/-}$ mice were cotreated with bosentan. WT vs. RKO, $p=0.49$, * ; RKO vs. RKO +C, $p =0.0001$, # ; RKO vs RKO+C+B, $p=0.11$, ^.

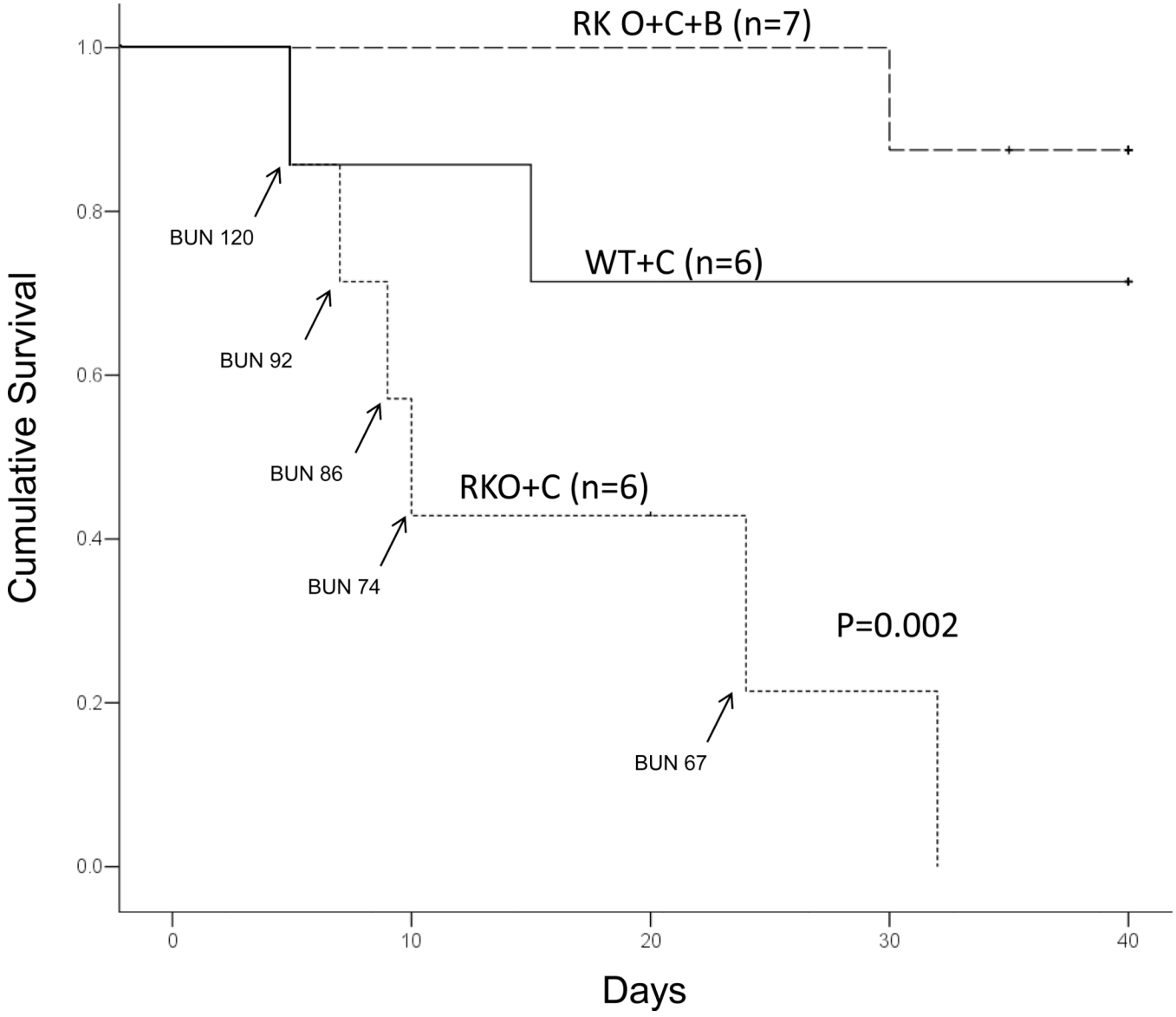

Figure 6.

Increased mortality after daily cyclosporine treatment in *rgs4*$^{-/-}$ mice (n=6) versus congenic wild type controls (n=6) treated with cyclosporine and *rgs4*$^{-/-}$ coadministered cyclosporine and bosentan (n=7). Survival with daily cyclosporine A treatment was monitored for 30 days (Mantel-Cox log rank test p=0.002).

7a

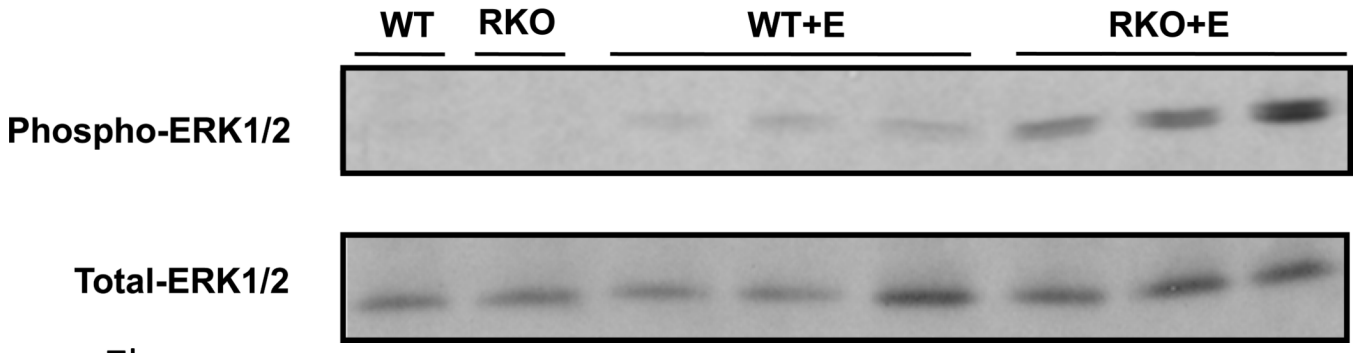

7b

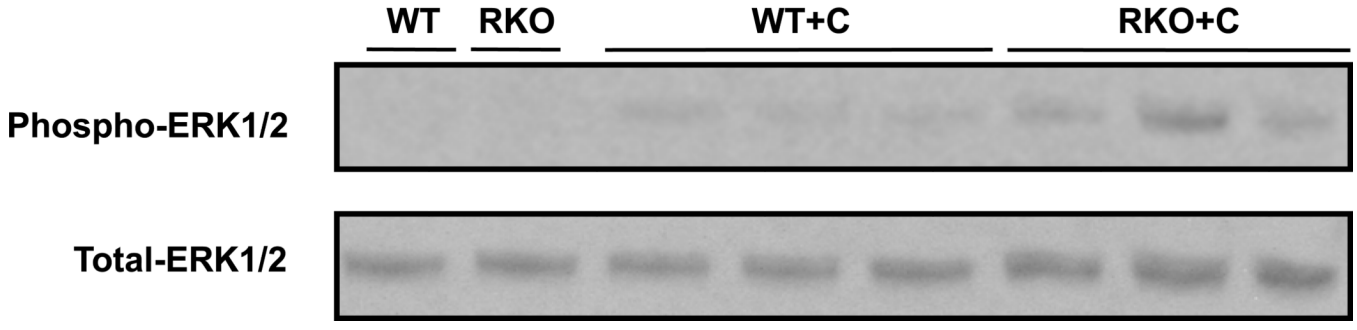

7 c,d

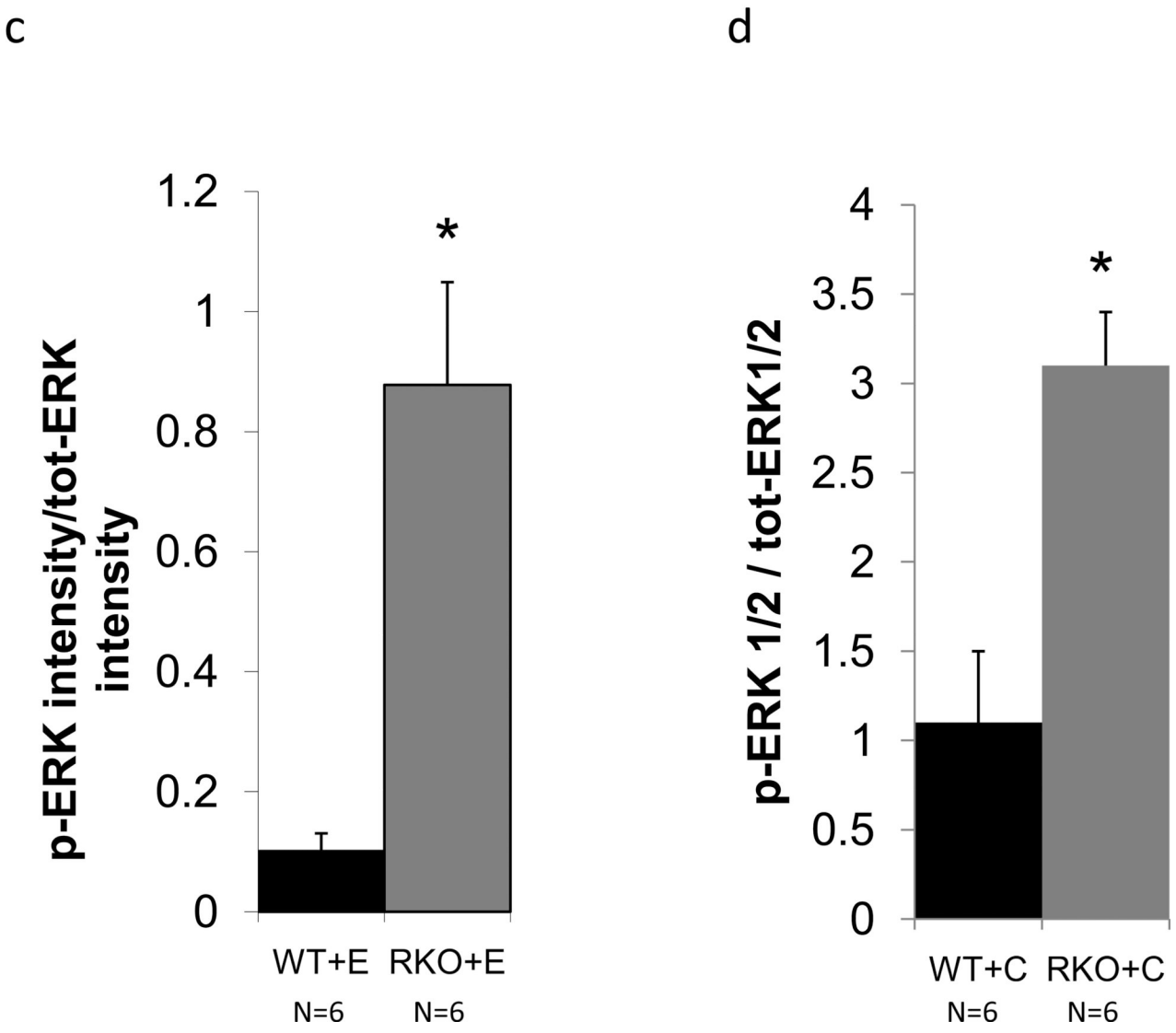

Figure 7.

In vitro and *in vivo* modulation of MAPK signaling in *rgs4*$^{-/-}$ after endothelin, or cyclosporine A treatment. Increased ERK1/2 activation in *rgs4*$^{-/-}$ kidney tissue after (**a,c**) endothelin-1 treatment ($p<0.0001$, *) and after (**b,d**) cyclosporine A treatment ($p=0.0003$, #). Kidneys were isolated from *rgs4*$^{-/-}$ (RKO) (n=6) and wild type congenic mice (WT) (n=6), quickly sliced into 2 mm sections and treated with endothelin-1 (E). Sections were used to generate protein lysates that were analyzed by anti-phospho-ERK1/2 immunobloting. Membranes were re-probed with an anti-total-ERK1/2 primary antibody to control for protein loading. Densitometric analysis of immunoreactive bands identified in Fig. 9 (a,b) was performed using Image J software 1.24.

8a

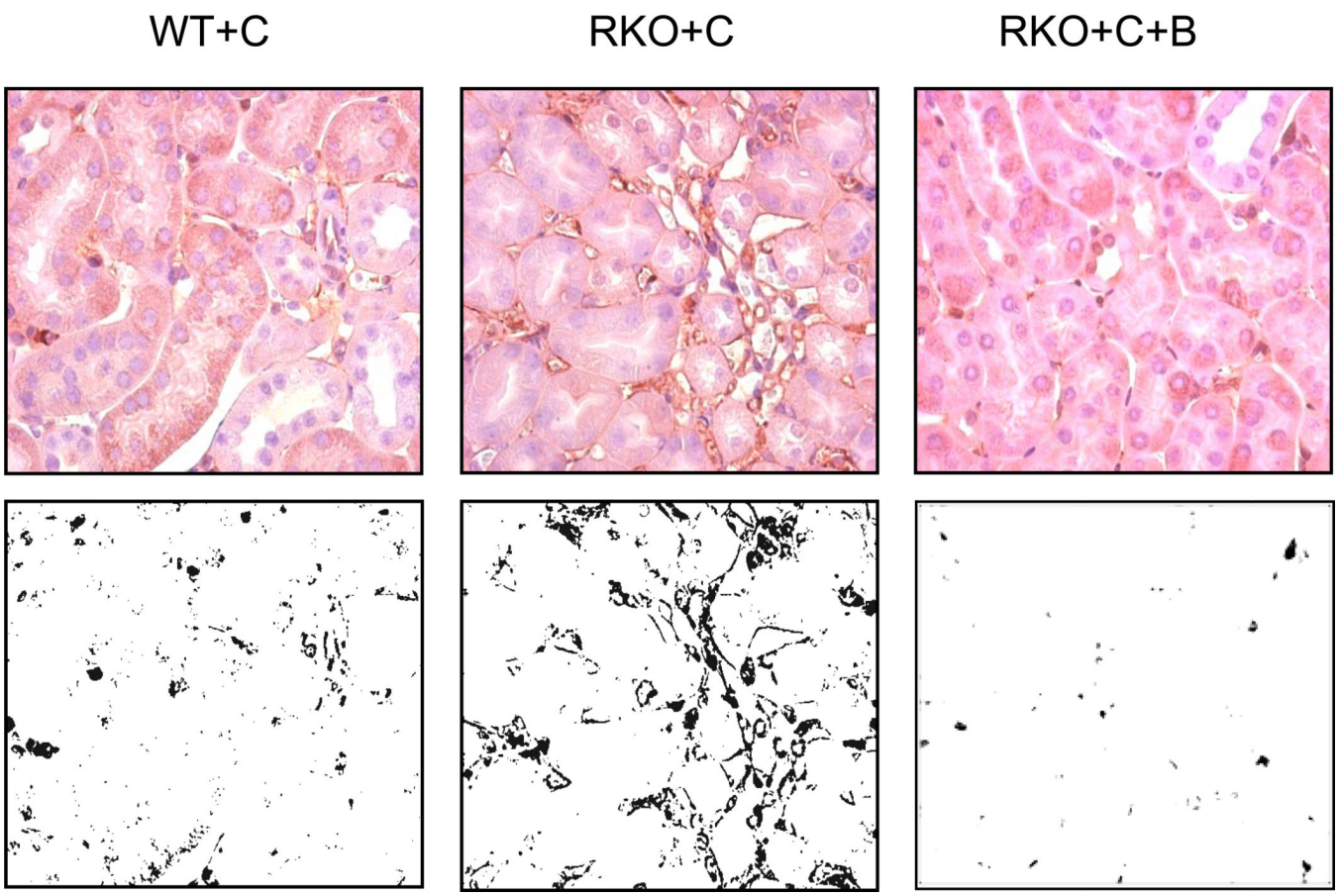

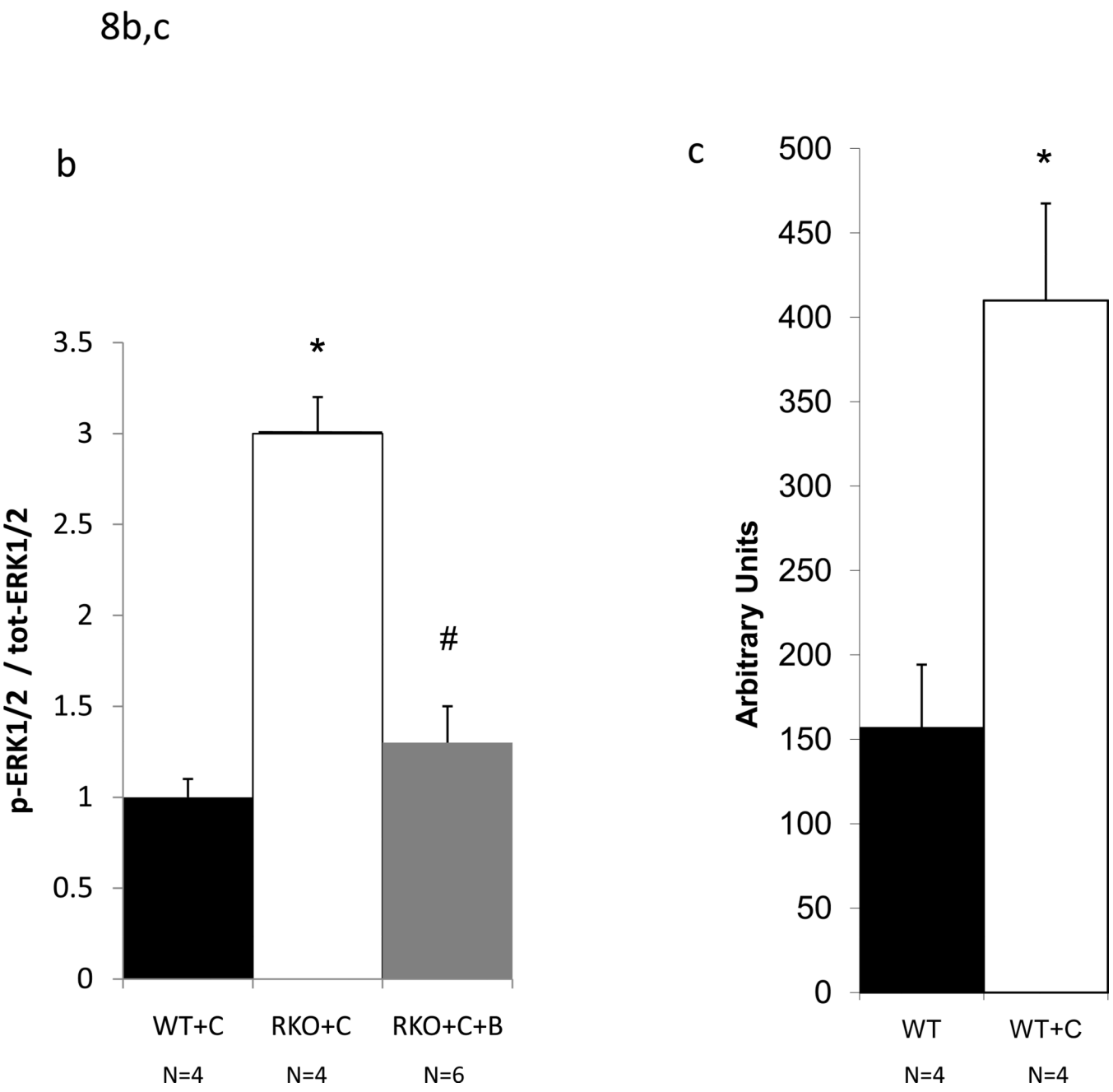

Figure 8.

ERK1/2 activation in *rgs4*$^{-/-}$ mice induced by cyclosporine A is inhibited after one week of cotreatment with bosentan. (**a**) After one week of daily cyclosporine A treatment, WT+C (n=4), RKO+C (n=4), and RKO+C+B (n=6) kidneys were isolated from wild type congenic mice *rgs4*$^{-/-}$ mice, fixed and embedded. Upper panels, embedded kidney tissue was analyzed by immunohistochemical staining with anti-phospho-ERK1/2 primary antibodies. Lower panels, digitized immunohistochemical images were converted to black-white contrast and analyzed with Image J software (**b**) to quantify ERK1/2 activation. ANOVA composite, p = <0.0001; WT+C vs RKO +C, p=0.0006, * ; RKO+C vs RKO+C+B, p=0<0.0001, #. (**c**) Increased renal RGS4 mRNA expression in wild type mice treated with C (n=4) for one week compared to untreated wild type mice. student's t-test, p=0.0003